

1 **The limited spatial scale of dispersal in soil arthropods revealed with**
2 **whole-community haplotype-level metabarcoding**

3 Arribas P^{1,2,3}, Andújar C^{1,2,3}, Salces-Castellano A¹, Emerson BC¹ & Vogler AP^{2,3}

4

5 ¹*Island Ecology and Evolution Research Group (IPNA-CSIC), Astrofísico Fco. Sánchez*
6 ³, 38206 La Laguna, Tenerife, Spain.

7 ²*Department of Life Sciences, Natural History Museum, Cromwell Road, London SW7*
8 ^{5BD, UK.}

9 ³*Department of Life Sciences, Imperial College London, Silwood Park Campus, Ascot*
10 ^{SL5 7PY, UK.}

11 *Corresponding author: Paula Arribas, pauarribas@ipna.csic.es.*

12

13 **RUNNING TITLE:** Limited scale of dispersal in soil mesofauna

14

15 **ABSTRACT**

16 Soil mesofauna communities are hyperdiverse and critical for ecosystem functioning.
17 However, our knowledge on spatial structure and underlying processes of community
18 assembly for soil arthropods is scarce, hampered by limited empirical data on species
19 diversity and turnover. We implement a high-throughput-sequencing approach to
20 generate comparative data for thousands of arthropods at three hierarchical levels:
21 genetic, species and supra-specific lineages. A joint analysis of the spatial arrangement
22 across these levels can reveal the predominant processes driving the variation in
23 biological assemblages at the local scale. This multi-hierarchical approach was performed
24 using haplotype-level-COI metabarcoding of entire communities of mites, springtails and
25 beetles from three Iberian mountain regions. Tens of thousands of specimens were

26 extracted from deep and superficial soil layers and produced comparative
27 phylogeographic data for >1000 co-distributed species and nearly 3000 haplotypes. Local
28 assemblages were highly distinctive between grasslands and forests, and within each of
29 them showed strong spatial structures and high endemism at the scale of a few kilometres
30 or less. The local distance-decay patterns were self-similar for the haplotypes and higher
31 hierarchical entities, and this fractal structure was very similar in all three regions,
32 pointing to a significant role of dispersal limitation driving the local-scale community
33 assembly. Our results from whole-community metabarcoding provide unprecedented
34 insight into how dispersal limitations constrain mesofauna community structure within
35 local spatial settings over evolutionary timescales. If generalized across wider areas, the
36 high turnover and endemism in the soil locally may indicate extremely high richness
37 globally, challenging our current estimations of total arthropod-diversity on Earth.

38

39

40 **KEYWORDS:** cMBC, dispersal, distance-decay, endemism, haplotype, soil
41 mesofauna, speciation scale.

42

43

44 INTRODUCTION

45 Soils are among the most biodiverse habitats on Earth, but represent probably the least
46 well studied, and thus poorly understood, terrestrial ecosystem (Bardgett & van der
47 Putten, 2014; Decaëns, 2010). Current understanding of terrestrial biodiversity has
48 mainly relied on studies of aboveground organisms, but in recent years efforts have been
49 focussed on developing an integrative understanding of soil biodiversity patterns and
50 underlying mechanisms (Thakur et al., 2019). However, current knowledge on soil
51 biodiversity is strongly unbalanced across taxonomic groups (Cameron et al., 2018),
52 which hampers the development of such integrative framework of soil biodiversity. In
53 particular, there is a pronounced shortage of basic biodiversity data, including estimations
54 of their species diversity and how it is spatially structured, for the taxonomically and
55 functionally diverse soil arthropod mesofauna composed of small-bodied invertebrates
56 measuring between 0.1 – 2 mm and found by thousands in virtually every square meter
57 of natural soil (Bardgett, Usher, & Hopkins, 2005; Decaëns, 2010). In recent years, high-
58 throughput sequencing has been applied widely to study the microbial components of soil
59 ecosystems and led to a solid understanding of global distribution patterns and the
60 ecological drivers of soil microbiomes (e.g. Delgado-Baquerizo et al., 2018; Ramirez et
61 al., 2018, 2014). In contrast, the study of soil arthropod mesofauna has seen
62 comparatively little progress in exploiting these tools (mostly using 18S eDNA
63 approaches Wu, Ayres, Bardgett, Wall, & Garey, 2011; Zinger et al., 2019), whereas
64 conventional taxonomic approaches have been onerous, given the small body size, limited
65 morphological variation and high local abundances of most mesofauna components.

66 Existing work on the diversity, distribution and community composition of soil
67 arthropods has focussed on springtails and oribatid mites, and mostly has pointed to
68 selection by abiotic and/or biotic environmental factors as major mechanisms of

69 community assembly at the local scale (e.g. Caruso, Trokhymets, Bargagli, & Convey,
70 2013; Magilton, Maraun, Emmerson, & Caruso, 2019; reviewed in Berg, 2012; Thakur
71 et al., 2019). Different studies have also reported purely spatial structures (independent
72 of the measured environmental variables) or stochastic patterns (non-environmental
73 neither spatial structures) for the soil mesofauna communities, that have been recurrently
74 attributed to the contribution of demographic processes (i.e., ecological drift without
75 dispersal limitation) in determining the local community assembly (Bahram, Kohout,
76 Anslan, Harend, & Abarenkov, 2016; Ingimarsdóttir et al., 2012; Widenfalk, Malmström,
77 Berg, & Bengtsson, 2016; Zinger et al., 2019). In addition, dispersal limitations have also
78 been suggested to contribute to some of the spatial community structures reported
79 (Caruso, Taormina, & Migliorini, 2012; Gao, He, Zhang, Liu, & Wu, 2014), but still is
80 rarely recognised as an important mechanism of assembly of the soil mesofauna at the
81 local scale (Berg, 2012; Thakur et al., 2019). Beyond the aggregated distribution within
82 the geographic ranges of the species, limitations to dispersal can determine the degree to
83 which species pools are differentiated over spatial distance (Hortal, Roura-Pascual,
84 Sanders, & Rahbek, 2010). These effects are frequently evident as biogeographic or
85 phylogeographic breaks at large (regional to continent-wide) scales, but if the scale of
86 movement is highly constrained and if the constraints are persistent through time, as could
87 be the case in the soil matrix, purely spatial patterns of community assemblage dominated
88 by species (and haplotype) turnover can arise even over relatively small distances. The
89 potentially low taxonomic resolution (due to morphological species assignment or the use
90 of 18S rRNA gene) of most of the studies on arthropod mesofauna communities may have
91 missed the importance of dispersal limitation in determining the diversity patterns of soil
92 mesofauna (but see Andújar et al., 2015; Lindo & Winchester, 2009).

93 The spatial scale at which dispersal constraints are effective in determining
94 species distributions and community assembly is a major “open question” in soil
95 biodiversity research (Thakur et al., 2019). For the mesofauna, small body size and high
96 local abundance may increase the probability of passive dispersal and long-distance
97 movement, and therefore dispersal constraints within the soil may be of limited
98 importance. In fact, a high prevalence of aerial, aquatic and marine rafting has been
99 demonstrated for various mesofaunal lineages (Coulson, Hodkinson, Webb, & Harrison,
100 2002; Nkem et al., 2006; Schuppenhauer, Lehmitz, & Xylander, 2019), and studies have
101 shown mesofaunal assemblages with no apparent dispersal limitation across continental-
102 scale areas (Baird, Leihy, Scheepers, & Chown, 2019), especially for the smallest-bodied
103 soil arthropods (Gan, Zak, & Hunter, 2019). On the other hand, molecular studies have
104 revealed high differentiation and ancient microendemism even in morphologically
105 indistinguishable clades, indicating long-term constraints to dispersal (Andújar, Pérez-
106 González, et al., 2017; Cicconardi, Fanciulli, & Emerson, 2013). These empirical data
107 limited to particular mesofauna lineages and their contrasting findings highlight the
108 difficulty of establishing the role of dispersal constraints in community assembly. As
109 such, inferences regarding the distribution and diversification of edaphic species, and thus
110 generalisations regarding macroecological and macroevolutionary patterns, remain
111 challenging.

112 New approaches to the study of diverse and cryptic arthropods using whole-
113 community metabarcoding (cMBC) using the mitochondrial COI gene are now
114 revolutionizing the understanding of complex arthropod communities (Arribas et al.,
115 2016; Ji et al., 2013). The methodology involves the bulk sequencing of mixed
116 communities and subsequent clustering of DNA reads into operational taxonomic units
117 (OTUs) that broadly represent the species category. While an efficient method to

118 approximate community profiles at the species-level, precise removal of primary DNA
119 reads affected by sequencing errors (Andújar, Arribas, Yu, Vogler, & Emerson, 2018;
120 Elbrecht, Vamos, Steinke, & Leese, 2018; Turon, Antich, Palacín, Præbel, &
121 Wangensteen, 2019) and co-amplified nuclear mitochondrial copies (numts) (Andújar et
122 al. under review) obviate the need for clustering. Read-based data raise the prospect of
123 reliable haplotype information from mitochondrial COI cMBC, which represents a step
124 change for the study of diversity patterns through whole-community genetic analyses at
125 haplotype-level resolution.

126 The availability of metabarcode data at both species and haplotype levels permits
127 the joint analysis of turnover (beta diversity) at different hierarchical levels, to assess
128 whether the variation in biological assemblages is predominantly driven by dispersal or
129 niche-based processes (Baselga et al., 2013; Baselga, Gómez-Rodríguez, & Vogler,
130 2015). Local assemblages may diverge simply due to the lack of population movement
131 which, when assessed for entire communities, results in a largely regular decay of
132 community similarity with spatial distance for the typically neutral haplotype variation of
133 the mitochondrial COI gene. Under a scenario where dispersal constraints determine the
134 spatial community structure, assemblage turnover at the species level should mirror these
135 haplotype patterns, albeit at a higher level of similarity. In contrast, niche-based processes
136 acting on species traits produce species distributions that mainly follow environmental
137 factors and thus differ from neutral conditions determining the haplotype distributions.
138 This confounds the correlation (self-similarity) of distance decay at the species and
139 haplotype levels, each driven by different processes, and thus the joint analysis of
140 communities at genetic and species levels provides a formal test to discern if a particular
141 spatial pattern of community assemblage is predominantly driven by dispersal (i.e.,
142 neutral) or niche-based processes (Baselga et al., 2013, 2015). In addition, multi-

143 hierarchical analyses may also describe the spatial scale at which dispersal constraints
144 act, and the variation of scale among different taxonomic groups or habitats (Gómez-
145 Rodríguez, Miller, Castillejo, Iglesias-Piñeiro, & Baselga, 2018; Múrria et al., 2017). This
146 framework remains to be exploited with whole-community mitochondrial cMBC.

147 Here we apply the multi-hierarchical framework to study the spatial structure of
148 entire assemblages of mites (Acari), springtails (Collembola) and beetles (Coleoptera)
149 including many thousands of specimens, in a semi-natural mosaic landscape within three
150 geographically distinct mountain regions in southern and central Iberia (Fig. 1 A). Our
151 aim was to generate rigorous whole-community data at haplotype, species (OTU) and
152 supra-specific levels to evaluate the spatial turnover at the local scale (i.e. <10 km,
153 following scale definitions of Pearson & Dawson, 2003) and in two habitat types within
154 the same spatial settings. Using the three regions as natural replicates, we evaluated
155 patterns of richness, endemism, turnover and the spatial scale of the distance decay in
156 community similarity at each hierarchical level and assessed the prevailing ecological and
157 evolutionary processes that determine the diversity and spatial distribution of soil
158 arthropod communities at the local scale.

159

160 **MATERIALS AND METHODS**

161 **Soil sampling and mesofauna extraction**

162 A total of 144 soil samples were collected from three regions in the southern Iberian
163 Peninsula at Sierra de Grazalema, (GRA), Sierra de Alatoz (ALZ) and Sierra de la
164 Alcarria Conquense (CUE) (Fig. 1 A). In each region, 24 points were sampled, half of
165 them in *Quercus* forest and half in wet grassland habitat, at distances of 500 m to a
166 maximum of 15 km (Fig. 1, Table S1). For each point, we collected i) a sample containing

167 the superficial soil layer (SUP), by extracting one square meter of leaf litter and humus
168 up to 5 cm deep and ii) a sample of the corresponding deep soil layer (DEEP), by
169 extracting the substrate of a 30 cm diameter core to 30 cm depth, comprising ca. 20 litres
170 of soil. Within each region and habitat, sampling points were located in natural patches
171 of similar dominant vegetation and elevation. Different variables characterising the
172 sampling points were recorded including elevation, slope, orientation, stoniness, humus
173 depth, qualitative porosity, roots, soil temperature and soil relative humidity (Table S1).

174 Superficial and deep soil samples were processed following the flotation–
175 Berlese–flotation protocol (FBF) of Arribas et al. (2016) for the ‘clean’ extraction of
176 arthropod mesofauna from a large volume of soil. Briefly, the FBF protocol is based on
177 the flotation of soil in water, which allows the extraction of the organic (floating) matter
178 containing the soil mesofauna from raw soil samples. Subsequently, the organic portion
179 is placed in a modified Berlese apparatus to capture specimens alive and preserve them
180 in absolute ethanol. The last part of the FBF protocol includes additional flotation and
181 filtering steps of the ethanol-preserved arthropods using 1-mm and 0.45- μ m wire mesh
182 sieves to remove debris and dirt accumulated in the Berlese extract. This procedure
183 generates two ‘clean’ subsamples of bulk specimens for DNA extraction, one including
184 all adult and larval Coleoptera, and a second with the smallest mesofauna typically
185 dominated by mites and springtails.

186 **DNA extraction, PCR amplification and Illumina sequencing**

187 Each bulk specimen subsample was independently homogenised and a DNA extraction
188 was performed using the DNeasy Blood and Tissue Spin-Column Kit (Qiagen). DNA
189 extracts were quantified using Nanodrop 8000 UV–Vis Spectrophotometer (Thermo
190 Scientific) and the corresponding subsample pairs were combined at a ratio of 1:10 in the
191 amount of DNA for Coleoptera to Acari plus Collembola (according to the range of

192 expected species diversity of these two fractions), in order to minimise the biomass bias
193 in the sequencing depth of the two mesofauna components. For metabarcoding, the bc3'
194 fragment corresponding to 418 bp of the 3' end of the COI barcode region was amplified.
195 Primers included a tail corresponding to the Illumina P5 and P7 sequencing adapters for
196 subsequent library preparation (see Arribas et al., 2016). For each sample, three
197 independent PCR reactions were performed and the amplicons were pooled. All
198 information regarding primers and PCR reagents and conditions is given in Table S2.
199 Amplicon pools were cleaned using Ampure XP magnetic beads, and used as template
200 for a limited-cycle secondary PCR amplification to add dual-index barcodes and the
201 Illumina sequencing adapters (Nextera XT Index Kit; Illumina, San Diego, CA, USA).
202 The resulting metabarcoding libraries were sequenced on an Illumina MiSeq sequencer
203 (2 x 300 bp paired-end reads) on ~ 1% of the flow cell each, to produce paired reads (R1
204 and R2) with a given dual tag combination for each sample. Negative controls were
205 maintained across all the different steps above and were sequenced as three independent
206 metabarcoding libraries.

207 **Bioinformatics read processing**

208 Raw reads were quality checked in Fastqc (Babraham Institute, 2013). Primers were
209 trimmed using fastx_trimmer and reads were processed in Trimmomatic (Bolger, Lohse,
210 & Usadel, 2014) using TRAILING:20. Based on results from (Andújar, Arribas, Gray, et
211 al., 2018) on the test of multiple tools and parameters for diverse metazoan metabarcoding
212 samples, we further processed each library independently following several steps of the
213 Usearch (Edgar, 2013) pipeline: reads were merged (option mergepairs --fastq_minovlen
214 50, -fastq_maxdiffs 15), quality-filtered (Maxee = 1), trimmed to full length amplicons
215 of 418 bp (-sortbylength), dereplicated (-fastx_uniques) and denoised (-unoise3, -minsize
216 4). Denoised reads from the 48 libraries for each region, representing putative haplotypes,

217 were combined and dereplicated to get a collection of unique sequences for each regional
218 dataset. The surviving reads were assigned to high-level taxonomic categories with the
219 lowest common ancestor (LCA) algorithm implemented in MEGAN V5 (Huson, Auch,
220 Qi, & Schuster, 2007). Each read was subjected to BLAST searches (blastn -outfmt 5 -
221 evaluate 0.001) against a reference library including the NCBI *nt* database (Accessed
222 December 2016) plus 382 sequences corresponding to Acari and Collembola collected at
223 Sierra de Grazalema. BLAST matches were fed into MEGAN to compute the taxonomic
224 affinity of each read. This high level taxonomic assignation allowed extracting reads
225 corresponding to the three target groups Acari, Collembola and Coleoptera, while
226 excluding other taxa present in the bulk samples. Reads corresponding to the target groups
227 were then aligned in Geneious using MAFFT and the Translation Align option, and those
228 with insertions, deletions or stop codons disrupting the reading frame were excluded.

229 Surviving haplotypes from each region were further filtered to remove likely
230 nuclear mitochondrial (numts) pseudogenes, following a protocol based on the relative
231 abundance of co-distributed reads (Andújar et al. under review). The set of putative
232 haplotypes for Acari, Collembola and Coleoptera was used to generate a community table
233 with read-counts (haplotype abundance) by sample against the complete collection of
234 reads (i.e., reads before the dereplicating and denoising steps) using Usearch (-
235 search_exact option). Using these abundances, we firstly removed from each library those
236 haplotypes with four or fewer reads according to the criteria used for the denoising (see
237 above). Next, we identified haplotypes that, in all the libraries where they were present,
238 contributed less than 1% of the total reads of the library. All reads falling in this category
239 were then removed from the analysis, as an auxiliary criterion to define spurious copies
240 not representing the true mitochondrial haplotypes. The 1% cut-off value removes most
241 of the spurious numts while maximizing the number of real haplotypes to be further

242 analysed (Andújar et al. under review). Community tables of fully filtered haplotypes
243 were then transformed into incidence (presence/absence) data, that added to the haplotype
244 filtering before, resulted in normalised samples for further analyses.

245 **Analysis of community composition and assembly at multiple thresholds of genetic** 246 **similarity**

247 The set of filtered haplotypes was used to generate an UPGMA tree with corrected genetic
248 distances (F84 model), and based on this tree all haplotypes were grouped into clusters of
249 genetic similarity at different thresholds (1%, 2%, 3%, 4%, 5%, 6% and 8%). This
250 grouping procedure based on patristic pairwise distances over a phylogenetic tree
251 including all haplotype sequences provided multiple hierarchical levels that each can be
252 used to estimate alpha diversity (Figure 1 provides a graphical abstract of the workflow).
253 These diversity measures were estimated for the richness of lineages by sample for the
254 whole mesofauna community but also for the subsets corresponding to Acari, Collembola
255 and Coleoptera. To test for significant differences in alpha diversity between the
256 communities of different habitats and soil layers of each sampling point, repeated-
257 measures ANOVAs were conducted using habitat and soil layer as grouping factors and
258 sampling point as a within-subjects factor. For each of the three local settings, total
259 accumulative richness (local scale richness) by habitat and soil layer and the contribution
260 of mites, springtails and beetles was also calculated for the various levels of genetic
261 similarity. Endemicity by sampling point was computed for each hierarchical level (once
262 DEEP and SUP samples were combined) as the lineages present exclusively at a single
263 sampling point in the region divided by the total number of lineages found in the region.
264 To assess whether the endemicity by sampling point differed between the communities
265 of forests and grasslands, Wilcoxon tests were conducted using habitat as a grouping
266 factor. For each of the three local settings, the local scale endemicity, defined as the

267 lineages present exclusively at a particular sampling point divided by the total number of
268 lineages in that community, was also calculated for the multiple levels of genetic
269 similarity.

270 For the multi-hierarchical assessment of the variation in community composition
271 at the local scale, the community dissimilarity matrices were generated for total beta
272 diversity (Sorensen index, β_{sor}) and its additive turnover (Simpson index, β_{sim}) and
273 nestedness (β_{sne}) components (Baselga, 2010), for each level of genetic similarity.
274 Community composition matrices were also used for non-parametric multidimensional
275 scaling (NMDS) and plots were created with the *ordispider* option to visualise the
276 compositional ordination of the communities according to the respective habitat and soil
277 layer. To assess for significant differences, permutational ANOVAs were conducted over
278 the community dissimilarity matrices using 999 permutations and the habitat and the soil
279 layer as grouping factors and sampling point as a within-subjects factor. The significant
280 relationships between the dissimilarity matrices generated for the Acari, Collembola and
281 Coleoptera were assessed independently by permutational multiple regression on distance
282 matrices (MRM), and additional NMDS ordinations and permutational ANOVAs as
283 before were in this case conducted for each taxonomic group.

284 The analysis of the variation in community composition with spatial distance
285 followed the ‘multi-hierarchical macroecology’ approach of (Baselga et al., 2013) which
286 is based on the joint analysis of distance decay of similarity patterns across the different
287 genetic levels. For each local setting and habitat, the relationship of community similarity
288 between pairs of points (1 – pairwise beta diversity, see above) with their spatial distance
289 (computed in kilometres as the Euclidean distance) was assessed independently at each
290 level of genetic similarity (from haplotypes to 8% lineages). A negative exponential
291 function was used to adjust a generalized linear model (GLM) with Simpson similarity as

292 response variable, spatial distance as predictor, log link and Gaussian error, and
293 maintaining the spatial distances untransformed (Gómez-Rodríguez & Baselga, 2018).
294 Finally, the existence of a fractal pattern (power law function) in the distance-decay
295 curves across the levels of genetic similarity was assessed by a log–log Pearson
296 correlation of genetic level and, independently: (a) number of lineages, (b) initial
297 similarity, and (c) mean similarity. High correlation values are indicative of self-
298 similarity in lineage branching (i.e., number of lineages) and/or spatial geometry of
299 lineage distributional ranges (i.e., initial and mean similarity, (Baselga et al., 2015), which
300 are predicted under a neutral process of community evolution.

301 In an equivalent way, these analyses were also conducted to assess the
302 relationships of community similarity and environmental distance as computed using
303 Gower's distance over the recorded variables characterising the sampling points (Table
304 S1). In the cases where this relationship was significant, variance partitioning was
305 conducted to assess the fractions of variance in community dissimilarity that are uniquely
306 and jointly explained by spatial and environmental distance. All analyses were performed
307 using the R-packages *vegan* (Oksanen et al., 2013), *cluster*, *PMCMR*, *hier.part*, *ecodist*,
308 and *betapart* (Baselga & Orme, 2012).

309

310 **RESULTS**

311 **Multi-hierarchical assessment of alpha and gamma diversity of soil mesofauna**

312 Processing of 144 soil samples using the FBF protocol, followed by double dual indexing
313 of *cox1* amplicons and Illumina MiSeq sequencing, produced 51433 to 375211 sequence
314 reads per sample for GRA, 11307 to 159244 for ALZ, and 43562 to 128149 for CUE.
315 Filtering of raw reads using standard protocols of read curation and denoising, followed

316 by removal of likely nuclear mitochondrial pseudogenes generated a conservative set of
317 clean sequences representing the mitochondrial haplotypes. A total of 1124, 1009 and 992
318 haplotypes were found for the GRA, ALZ and CUE local areas respectively, and these
319 numbers declined rapidly when haplotypes were grouped at increasing threshold values,
320 e.g. 511, 479 and 480 lineages at 3% similarity (Table 1), but they declined only slightly
321 further at the higher thresholds, indicating the point at which stable groups are obtained
322 that broadly represent the species level. The relative proportions of mites, springtails and
323 beetles were similar across the three local settings and hierarchical levels, with Acari
324 representing the richest group (around the 50% of clusters) followed by Collembola and
325 Coleoptera in similar proportions (Table 1).

326 The patterns of richness by sample (alpha diversity) for the different habitats, soil
327 layers and genetic thresholds were similar for the three regions, with mean values between
328 35 - 60 haplotypes and 25 - 42 lineages at 3% per sample (Fig. 2 A, B, C and Fig. S1).
329 Superficial soils had significantly higher diversity than their corresponding deep soil
330 counterparts for the overall dataset and for both of the forest and grassland habitats
331 assessed independently (Fig. 2 A, B, C, Fig S1 and Table S3). At GRA, forest habitat
332 showed significantly higher alpha diversity per sample than grassland but no significant
333 differences between forest and grassland were found for ALZ and CUE (Fig. 2 A, B, C
334 and Fig S1, Table S3).

335 The local-scale cumulative richness at each region (gamma diversity) showed
336 more diverse communities for the superficial compared with deep layers, and gamma
337 diversity was generally higher for forest than grassland habitats, but the differences
338 between both habitat types were lower than observed for alpha diversity. Thus, species
339 accumulation was higher for the grassland than forest habitats, and the grassland
340 superficial layers had the highest total richness of haplotypes for ALZ and CUE, and the

341 highest for the three regions at the 3% similarity level (Fig. 2 D, E, F and Fig S2). Patterns
342 of alpha and gamma diversity for the subsets of mites, springtails and beetles were similar
343 (Fig. S2 and S3).

344 **Multi-hierarchical assessment of beta diversity and endemism of soil mesofauna**

345 Compositional dissimilarity of communities within each of the three regions was high
346 and was dominated by lineage turnover β_{sim} , instead of nestedness β_{sne} ($0.8 > \beta_{sim} > 0.95$),
347 across all hierarchical levels. NMDS showed a consistent pattern of the forest and
348 grassland habitats as the main driver of the ordination while soil layers had a secondary
349 role (Fig. 3, Fig. S4). Accordingly, for the three regions and all genetic levels, the
350 community composition was significantly different for both habitats and soil layers but
351 the proportion of variance explained by the forest-grassland factor was always higher
352 (Fig. 3 and Table S4). Beta diversity matrices for mites, springtails and beetles showed
353 high and significant correlations for each of the genetic similarity levels (Table S5), and
354 when independently analysed, these main taxonomic groups each showed similar patterns
355 of community composition.

356 Community similarity (1-pairwise beta diversity) significantly decreased with
357 spatial distance (distance decay) at all levels of genetic similarity for both the forest and
358 grassland habitats, and these patterns were remarkably consistent across the three local
359 settings (Fig. 4, Table S6). The slopes of the exponential decay curves were very similar
360 at all threshold levels, and assemblage similarity increased with each level (Fig. 4, Table
361 S6). The levels of genetic similarity showed a high and significant log–log correlation
362 with the number of lineages ($0.90 < r^2 > 0.96$, $p < 0.001$), initial similarity ($0.86 < r^2 >$
363 0.96 , $p < 0.001$) and mean similarity of communities ($0.89 < r^2 > 0.95$, $p < 0.001$) for all
364 three regions and two habitats, as expected if community variation across genetic
365 similarity levels can be described by a fractal geometry (Baselga et al., 2013, 2015).

366 Comparisons of distance-decay relationships between forests and grasslands
367 showed similar values for explained variance and for the slopes for the three regions (Fig.
368 4, Table S6). However, there was a consistent pattern of a lower initial community
369 similarity in grasslands than in forests, particularly above the haplotype level (Fig. 4).
370 Similarly, the local-scale (mean) dissimilarity of communities was always higher for
371 grasslands than for forests and the differences between both increased across the levels
372 of genetic similarity (Fig. 5 A, B, C). A decrease in community similarity with
373 environmental distance was only significant in the case of the forests from ALZ and CUE,
374 but variance partitioning showed that uniquely explained variance in environmental
375 distance, i.e. independently of the spatial distance, was reduced (5 – 9 % of explained
376 variation at all levels) compared with the uniquely explained variance in spatial distance
377 (23 – 31 % of explained variation).

378 The endemism within the GRA, ALZ and CUE regions ranged from 71%, 64%
379 and 58% at the haplotype level to 55%, 53% and 46% for lineages at the 3% threshold,
380 respectively (Table 1). Comparisons between forest and grassland habitats showed that
381 the local scale endemism of grassland communities was higher in the case of GRA and
382 CUE but similar in both habitats for ALZ (Fig. 5 D, E, F). The endemism by sampling
383 points was consistently higher for grassland than for forest local communities particularly
384 above the haplotype level, but the differences were significant only in the case of the
385 GRA localities (Fig. 5 G, H, I).

386

387 **DISCUSSION**

388 In total, soil samples from three Iberian mountain regions produced over 1000 species
389 and nearly 3000 haplotypes. Their distribution was determined across numerous sampling
390 points, demonstrating the power of mitochondrial cMBC to overcome previous

391 impediments to studying the arthropod mesofauna of the soil using conventional
392 morphological and molecular approaches. Data analysis in a multi-hierarchical
393 framework revealed a strong spatial community structure and high levels of endemism
394 at haplotype, species and supra-specific levels, even at sampling points that were mostly
395 within a few kilometres of each other (maximum 15 km). Patterns of turnover and
396 endemism were similar in all three independent study regions and in the grassland and
397 forest biomes (that each harbour largely non-overlapping communities). Distance decay
398 is evident at all hierarchical levels, and can be described as self-similar. The coincidence
399 of community turnover at population level and species level is expected if soil arthropod
400 assemblages are predominantly driven by distance-based parameters, if movement is
401 strongly constrained at the local scale and over time. In addition, the overriding
402 importance of habitat-related processes was apparent from the strong differentiation of
403 grassland and forest communities, which again was seen recurrently in each of the three
404 study regions.

405 The study extends existing comparative analyses of soil mesofauna by improving
406 the taxonomic resolution, providing haplotype level variation and spanning most lineages
407 composing the soil arthropod communities. Broad surveys of invertebrate soil diversity
408 using HTS have commonly relied on markers of low species-level resolution and via
409 eDNA extracted from small soil samples (Bahram et al., 2016; Wu et al., 2011; Zinger et
410 al., 2019). Other studies have characterise specific groups of mites or springtails by
411 individualised processing of specimens and relying on morphological assignment to
412 generate species-level data (Caruso, Schaefer, Monson, & Keith, 2019; Ingimarsdóttir et
413 al., 2012), but see also Young, Proctor, DeWaard, & Hebert (2019) on molecular species
414 assignment. HTS data now greatly increase the potential of expanding both the number
415 of species studied and the level of detail at which intra-specific variation for each is

416 captured. To our knowledge, this is the first study that provides haplotype level data for
417 entire communities (one square meter of leaf litter and humus and ca. 20 litres of soil per
418 sampling point) of the three most species rich soil arthropods, which allows surveys of
419 community composition and species turnover at an unprecedented level of detail, both
420 spatially and genetically. With this data in hand, community level responses to distance-
421 based parameters can be assessed that may be not evident in other types of studies. In
422 addition, the combined haplotype and species level data permit the exploitation of the
423 hierarchical framework of Baselga et al. (2013, 2015) for discriminating between
424 distance- and niche-based factors of community assembly.

425 ***The limited spatial scale of dispersal in soil arthropods***

426 The literature exploring the community assemblage of arthropod mesofauna at the local
427 scale is generally arguing for the selection by abiotic and/or biotic environmental factors
428 as the predominant mechanisms (see Berg, 2012; Thakur et al., 2019 for a recent review)
429 but stochastic and purely spatial patterns have also been reported, pointing to a
430 contribution of dispersal and demographic processes at least in some local settings
431 (Caruso et al., 2012; Gao et al., 2014; Gao, Liu, Lin, & Wu, 2016; Zinger et al., 2019).
432 However, strong dispersal constraints have rarely been recognised as an important
433 mechanism of soil mesofauna assembly at the local scale, and this could be in part due to
434 the potentially low taxonomic resolution of most of the community-level studies in this
435 group that used morphological or 18S rRNA gene species assignment (see Tang et al.,
436 2012 on the low taxonomic resolution of this marker). Our results demonstrate high
437 community differentiation at the kilometre scale for both genetic and species levels. The
438 key observation from the multi-hierarchical analysis is the correlated distance decay at
439 haplotype and species level. Self-similarity is expected to be eroded by selection on
440 adaptive traits at the species level, but not at the (neutral) haplotype level (Baselga et al.,

441 2015; Gómez-Rodríguez et al., 2018). As the data largely confirm the self-similarity of
442 distance decay at haplotype and species level, this is interpreted to support the
443 predominant role of dispersal limitation driving community assembly. The predominance
444 of the dispersal constraints seems to emerge at short spatial distances within the soil
445 matrix, and the evident high turnover with physical distance suggests that our sampling
446 within each study regions (local scale) is beyond the scale of a single metacommunity.
447 Short dispersal distances probably have affected a significant proportion of lineages
448 within these communities over evolutionary timescales in a largely stable spatial setting.
449 The spatiotemporal continuum expected under this scenario predicts that lineages in more
450 distant places have diverged at a more distant time point in evolutionary history (Baselga
451 et al., 2013, 2015), and our findings of a largely regular distance decay at higher levels
452 are consistent with this prediction. Additional evidence for the role of short dispersal
453 distance driving the local community assembly comes from the high microendemism
454 found at all hierarchical levels, an overall picture which is not expected under a scenario
455 with predominant environmental drivers nor ecological drift without dispersal limitation.

456 Yet, the influence of environmental drivers cannot be discarded entirely. Even if
457 the recorded environmental variables did not explain the variation in community
458 composition, a significant portion of the unexplained variance in the distance-decay
459 curves potentially suggests the influence of non-spatial factors determining the
460 community composition. Edaphic parameters such as soil pH or organic matter have been
461 shown to explain a significant part of the variance observed in the distribution of the soil
462 mesofauna communities (Caruso et al., 2012; Gao et al., 2014), and here could be driving
463 at least part of the unexplained variation within the different habitats and regions. Edaphic
464 environmental variables are often spatially structured and so have been also reported as
465 potential drivers of purely spatial patterns in mesofauna communities (Caruso et al., 2019,

466 2012). However as exposed before, this possibility is poorly supported here, as similar
467 spatial structures were independently found within the different habitats and regions,
468 mirroring the distance-decay patterns at the (neutral) haplotype level, and hence
469 suggesting that dispersal limitation is the main driver of the local spatial structure of the
470 studied mesofauna communities.

471 The small spatial scale of turnover and endemism is consistent with population
472 genetic studies in soil mesofauna showing deep genetic breaks even over relative short
473 geographic distances (Andújar, Pérez-González, et al., 2017; Cicconardi et al., 2013). In
474 contrast, our results are not concordant with the extended view of long-distance dispersal
475 as prevalent process for soil mesofauna, as might be expected from evidences of passive
476 dispersal by air, water or in marine plankton (Decaëns, 2010; Thakur et al., 2019; Wardle,
477 2002). Existing reports of long-distance dispersal are mainly into virgin isolated habitats
478 (Ingimarsdóttir et al., 2012) or recently deglaciated areas (Gan et al., 2019), or may
479 involve the detection of mesofauna during transport (Coulson, Hodkinson, & Webb,
480 2003; Schuppenhauer et al., 2019). However, they do not inform about colonisation and
481 establishment success (effective dispersal) and possibly only pertain to a few highly
482 dispersive species. Additionally, the dispersal potential may have been overestimated due
483 to the low resolution of morphological species identification (Cicconardi et al., 2013)
484 leading to perceived low turnover among sites, as evident from recent large-scale
485 barcoding studies (Young et al., 2019). Our results at the community level thus raise
486 doubts about a generalised dispersal advantage for small-bodied arthropods and instead
487 indicate very small dispersal distances, even over evolutionary time scales, for the
488 majority of species that make up the complex mesofauna communities of the soil. This
489 scale and dynamics of community assembly contrasts with patterns and processes
490 reported for the microbial eukaryote diversity of the soil (Bahram et al., 2016) and aligns

491 with recent empirical evidences suggesting that at the local scale dispersal rates may be
492 much lower for soil mesofauna than for microfauna (Zinger et al., 2019). In the context
493 of the overall arthropod diversity (for which soil mesofauna comprises the majority of the
494 smallest fraction), our results are not supporting the macroecological prediction for a
495 reduce impact of dispersal limitation in the assemblage for small-bodied components
496 compared with their bigger counterparts (de Bie et al., 2012; Ricklefs, 2004) and highlight
497 the uniqueness of ecological and evolutionary processes driving the biodiversity of these
498 edaphic arthropods (Andújar, Arribas, & Vogler, 2017; Andújar, Pérez-González, et al.,
499 2017).

500 *The role of dispersal constraints within a habitat-based framework*

501 In spite of the evidence for an important role for dispersal limitation within each habitat
502 type, the greatest effect was the differentiation of grassland and forest communities,
503 which share very few species even in close (meters) spatial proximity. Previous studies
504 also have shown great differences in soil arthropod community composition between
505 beech forest and adjacent grassland (Caruso et al., 2012), and twice higher species
506 richness in the forest community. The grassland-forest dichotomy in community
507 composition is concordant with these findings, but the total diversity in either type of
508 community was more complex: alpha diversity tended to be higher for forest habitats, but
509 lineage accumulation across multiple sites was higher for the grasslands, resulting in
510 higher overall landscape richness (gamma diversity). Grassland communities also had
511 consistently lower initial and mean community similarities in the corresponding distance
512 decay curves, together with higher levels of both point and local scale endemism. These
513 results are recurrent across the three sampling areas and point to slightly higher long-term
514 dispersal constraints for the mesofauna in the grasslands studied.

515 Grassland species are expected to experience higher environmental variability and
516 greater extremes, which are moderated within forested patches and thus are presumably
517 more stable (De Frenne et al., 2019). Under the habitat stability hypothesis (Ribera &
518 Vogler, 2000; Southwood, 1977), low species turnover is predicted in less stable habitats
519 due to the stronger positive selection on traits promoting dispersal that are required to
520 persist in ephemeral environments. However, our findings are not aligned with this
521 hypothesis, suggesting similar local-scale patterns of lineage turnover within both
522 habitats and with slightly stronger community structure for the presumably less stable
523 grasslands. Further studies comparing the assemblages of both habitat types across
524 gradients of stability (e.g. latitude) are fundamental to identify the similarities and
525 disparities in the processes driving the diversity and structure of the mesofauna
526 communities. Regardless of the potential differences between the two habitat types, the
527 high overall turnover suggests the long-term stability of the soil environment without
528 which the high spatial structure at multiple hierarchical levels and between grassland and
529 forest habitats could not have arisen.

530 *Extrapolating beyond the local scale*

531 Disentangling the mechanisms at larger spatial scales might be challenging without the
532 understanding of the underlying processes at relatively fine scales. The recurrence of the
533 local patterns in each of the three study regions and across the three major taxonomic
534 groups, corroborates the hypothesis of an underlying process of stochastic dispersal of
535 individuals, affected by a universal type of dispersal constraint. This seems to affect to a
536 majority of the soil arthropod fauna composing these communities, regardless of their
537 taxonomic affinity, species traits or functional role. The soil matrix provides a common
538 sphere in which these processes are played out, and if these soils are similar, complex
539 communities, on average, appear to respond in a similar way. The two habitat types

540 clearly provide a different overall setting, obvious from the very different species present,
541 but they also impact the respective species pool in similar ways. With the local-scale
542 patterns and likely underlying processes reported here, questions arise about the impact
543 for cross-regional and global spatial scales, and how these patterns and processes compare
544 to aboveground arthropod components. If generalized across broader geographical scales
545 and latitudes, the proposed process of a very reduced spatial scale of dispersal in soil
546 mesofauna communities could be a major contribution to the overall gamma diversity of
547 ecosystems and would suppose a great underestimation of global diversity on Earth. In
548 this sense, further developments on the multi-hierarchical analysis of genetic and higher-
549 level diversity from metabarcoding data has the potential to propel the characterisation of
550 edaphic microbial community structure into a new era of biodiversity discovery. By
551 taking advantage of the full breadth of contemporary metabarcoding data at
552 unprecedented taxonomic and geographic scales, the advances made here will be able to
553 provide unique insights into the ecological and evolutionary processes that determine the
554 magnitude and spatial distribution of soil arthropods.

555

556 **ACKNOWLEDGMENTS**

557 This research was funded by Newton International Program, UK to PA and the NHM
558 Biodiversity Initiative to APV. PA was supported by two postdoctoral grants from the
559 Royal Society (Newton International Program, UK) and the Spanish Ministry of
560 Economy and Competitiveness (MINECO, Spain) within the Juan de la Cierva
561 Formación Program. CA was supported by the Spanish Ministry of Economy and
562 Competitiveness (MINECO, Spain) (CGL2015-74178-JIN). Thanks are due to the
563 regional government of Andalucía and Castilla-la-Mancha (Spain); Alex Aitken, Andie
564 Hall, Stephen Russell and Peter Foster (all NHM) for their technical assistance and to

565 Jesús Arribas who assisted with field sampling.

566

567 REFERENCES

- 568 Andújar, C., Arribas, P., Gray, C., Bruce, C., Woodward, G., Yu, D. W., & Vogler, A.
569 P. (2018). Metabarcoding of freshwater invertebrates to detect the effects of a
570 pesticide spill. *Molecular Ecology*, 27(1), 146–166. doi: 10.1111/mec.14410
- 571 Andújar, C., Arribas, P., Ruzicka, F., Platt, A. C., Timmermans, M. J. T. N. M. J. T. N.
572 J. T. N., Vogler, A. P. A. A. P., ... Vogler, A. P. A. A. P. (2015). Phylogenetic
573 community ecology of soil biodiversity using mitochondrial metagenomics.
574 *Molecular Ecology*, 24(14), 3603–3617. doi: 10.1111/mec.13195
- 575 Andújar, C., Arribas, P., & Vogler, A. P. (2017). Terra incognita of soil biodiversity:
576 unseen invasions under our feet. *Molecular Ecology*, 26(12), 3087–3089. doi:
577 10.1111/mec.14112
- 578 Andújar, C., Arribas, P., Yu, D. W., Vogler, A. P., & Emerson, B. C. (2018). Why the
579 COI barcode should be the community DNA metabarcode for the Metazoa.
580 *Molecular Ecology*, 27(July), 3968–3975. doi: 10.1111/mec.14844
- 581 Andújar, C., Pérez-González, S., Arribas, P., Zaballos, J. P., Vogler, A. P., & Ribera, I.
582 (2017). Speciation below ground: Tempo and mode of diversification in a radiation
583 of endogean ground beetles. *Molecular Ecology*, 26(21), 6053–6070. doi:
584 10.1111/mec.14358
- 585 Arribas, P., Andújar, C., Hopkins, K., Shepherd, M., Vogler, A. P., Andújar, C., ...
586 Vogler, A. P. A. P. (2016). Metabarcoding and mitochondrial metagenomics of
587 endogean arthropods to unveil the mesofauna of the soil. *Methods in Ecology and*
588 *Evolution*, 7(9), 1071–1081. doi: 10.1111/2041-210X.12557
- 589 Babraham Institute. (2013). *FastQC: A quality control tool for high throughput*
590 *sequence data*. <http://www.bioinformatics.babraham.ac.uk/projects/fastqc>.
- 591 Bahram, M., Kohout, P., Anslan, S., Harend, H., & Abarenkov, K. (2016). Stochastic
592 distribution of small soil eukaryotes resulting from high dispersal and drift in a
593 local environment. *ISME Journal*, 10(4), 885–896. doi: 10.1038/ismej.2015.164
- 594 Baird, H. P., Leihy, R. I., Scheepers, C. J., & Chown, S. L. (2019). The ecological
595 biogeography of indigenous and introduced Antarctic springtails. *Journal of*
596 *Biogeography*, (April), 1–15. doi: 10.1111/jbi.13639
- 597 Bardgett, R. D., Usher, M. B., & Hopkins, D. W. (2005). *Biological diversity and*
598 *function in soils*. Cambridge: Cambridge University Press.
- 599 Bardgett, R. D., & van der Putten, W. H. (2014). Belowground biodiversity and
600 ecosystem functioning. *Nature*, 515(7528), 505–511. doi: 10.1038/nature13855
- 601 Baselga, A. (2010). Partitioning the turnover and nestedness components of beta
602 diversity. *Global Ecology and Biogeography*, 19(1), 134–143. doi: 10.1111/j.1466-
603 8238.2009.00490.x
- 604 Baselga, A., Fujisawa, T., Crampton-Platt, A., Bergsten, J., Foster, P. G., Monaghan, M.

- 605 T., & Vogler, A. P. (2013). Whole-community DNA barcoding reveals a spatio-
606 temporal continuum of biodiversity at species and genetic levels. *Nature*
607 *Communications*, 4(May), 1892. doi: 10.1038/ncomms2881
- 608 Baselga, A., Gómez-Rodríguez, C., & Vogler, A. P. (2015). Multi-hierarchical
609 macroecology at species and genetic levels to discern neutral and non-neutral
610 processes. *Global Ecology and Biogeography*, 873–882. doi: 10.1111/geb.12322
- 611 Baselga, A., & Orme, C. D. L. (2012). betapart : an R package for the study of beta
612 diversity. *Methods in Ecology and Evolution*, 3(5), 808–812. doi: 10.1111/j.2041-
613 210X.2012.00224.x
- 614 Berg, M. P. (2012). Patterns of biodiversity at fine and small spatial scales. In D. H.
615 Wall, R. D. Bardgett, V. M. Behan-Pelletier, & E. Al. (Eds.), *Soil Ecology and*
616 *Ecosystem Services* (pp. 136–152). Oxford: Oxford University Press.
- 617 Bolger, A. M., Lohse, M., & Usadel, B. (2014). Trimmomatic: A flexible trimmer for
618 Illumina sequence data. *Bioinformatics*, 30(15), 2114–2120. doi:
619 10.1093/bioinformatics/btu170
- 620 Cameron, E. K., Martins, I. S., Lavelle, P., Mathieu, J., Tedersoo, L., Gottschall, F., ...
621 Eisenhauer, N. (2018). Global gaps in soil biodiversity data. *Nature Ecology and*
622 *Evolution*, 2(7), 1042–1043. doi: 10.1038/s41559-018-0573-8
- 623 Caruso, T., Schaefer, I., Monson, F., & Keith, A. M. (2019). Oribatid mites show how
624 climate and latitudinal gradients in organic matter can drive large-scale
625 biodiversity patterns of soil communities. *Journal of Biogeography*, 46(3), 611–
626 620. doi: 10.1111/jbi.13501
- 627 Caruso, T., Taormina, M., & Migliorini, M. (2012). Relative role of deterministic and
628 stochastic determinants of soil animal community: a spatially explicit analysis of
629 oribatid mites. *The Journal of Animal Ecology*, 81(1), 214–221. doi:
630 10.1111/j.1365-2656.2011.01886.x
- 631 Caruso, T., Trokhymets, V., Bargagli, R., & Convey, P. (2013). Biotic interactions as a
632 structuring force in soil communities: Evidence from the micro-arthropods of an
633 Antarctic moss model system. *Oecologia*, 172(2), 495–503. doi: 10.1007/s00442-
634 012-2503-9
- 635 Cicconardi, F., Fanciulli, P. P. P., & Emerson, B. C. B. (2013). Collembola, the
636 biological species concept and the underestimation of global species richness.
637 *Molecular Ecology*, 22(21), 5382–5396. doi: 10.1111/mec.12472
- 638 Coulson, S. J., Hodkinson, I. D., & Webb, N. R. (2003). Microscale distribution patterns
639 in high Arctic soil microarthropod communities: The influence of plant species
640 within the vegetation mosaic. *Ecography*, 26(6), 801–809. doi: 10.1111/j.0906-
641 7590.2003.03646.x
- 642 Coulson, S. J., Hodkinson, I. D., Webb, N. R., & Harrison, J. A. (2002). *Survival of*
643 *terrestrial soil-dwelling arthropods on and in seawater : implications for trans-*
644 *oceanic dispersal*. 353–356.

- 645 de Bie, T., de Meester, L., Brendonck, L., Martens, K., Goddeeris, B., Ercken, D., ...
646 Declerck, S. A. . (2012). Body size and dispersal mode as key traits determining
647 metacommunity structure of aquatic organisms. *Ecology Letters*, *4*, 740–747. doi:
648 10.1111/j.1461-0248.2012.01794.x
- 649 De Frenne, P., Zellweger, F., Rodríguez-Sánchez, F., Scheffers, B. R., Hylander, K.,
650 Luoto, M., ... Lenoir, J. (2019). Global buffering of temperatures under forest
651 canopies. *Nature Ecology and Evolution*, *3*(5), 744–749. doi: 10.1038/s41559-019-
652 0842-1
- 653 Decaëns, T. (2010). Macroecological patterns in soil communities. *Global Ecology and*
654 *Biogeography*, *19*(3), 287–302. doi: 10.1111/j.1466-8238.2009.00517.x
- 655 Delgado-Baquerizo, M., Oliverio, A. M., Brewer, T. E., Benavent-gonzález, A.,
656 Eldridge, D. J., Bardgett, R. D., ... Fierer, N. (2018). Bacteria Found in Soil.
657 *Science*, *325*(February), 320–325. doi: 10.1126/science.aap9516
- 658 Edgar, R. C. (2013). UPARSE: highly accurate OTU sequences from microbial
659 amplicon reads. *Nature Methods*, *10*(10), 996–998. doi: 10.1038/nmeth.2604
- 660 Elbrecht, V., Vamos, E. E., Steinke, D., & Leese, F. (2018). Estimating intraspecific
661 genetic diversity from community DNA metabarcoding data. *PeerJ*, *6*, e4644. doi:
662 10.7717/peerj.4644
- 663 Gan, H., Zak, D. R., & Hunter, M. D. (2019). Scale dependency of dispersal limitation,
664 environmental filtering and biotic interactions determine the diversity and
665 composition of oribatid mite communities. *Pedobiologia*, *74*(June 2017), 43–53.
666 doi: 10.1016/j.pedobi.2019.03.002
- 667 Gao, M., He, P., Zhang, X., Liu, D., & Wu, D. (2014). Relative roles of spatial factors,
668 environmental filtering and biotic interactions in fine-scale structuring of a soil
669 mite community. *Soil Biology and Biochemistry*, *79*, 68–77. doi:
670 10.1016/j.soilbio.2014.09.003
- 671 Gao, M., Liu, D., Lin, L., & Wu, D. (2016). The small-scale structure of a soil mite
672 metacommunity. *European Journal of Soil Biology*, *74*, 69–75. doi:
673 10.1016/j.ejsobi.2016.03.004
- 674 Gómez-Rodríguez, C., & Baselga, A. (2018). Variation among European beetle taxa in
675 patterns of distance decay of similarity suggests a major role of dispersal
676 processes. *Ecography*, *41*(11), 1825–1834. doi: 10.1111/ecog.03693
- 677 Gómez-Rodríguez, C., Miller, K. E., Castillejo, J., Iglesias-Piñero, J., & Baselga, A.
678 (2018). Understanding dispersal limitation through the assessment of diversity
679 patterns across phylogenetic scales below the species level. *Global Ecology and*
680 *Biogeography*, (October), 1–12. doi: 10.1111/geb.12857
- 681 Hortal, J., Roura-Pascual, N., Sanders, N. J., & Rahbek, C. (2010). Understanding
682 (insect) species distributions across spatial scales. *Ecography*, *33*(1), 51–53. doi:
683 10.1111/j.1600-0587.2009.06428.x
- 684 Huson, D. H., Auch, A. F., Qi, J., & Schuster, S. C. (2007). MEGAN analysis of

- 685 metagenomic data. *Genome Research*, 17(3), 377–386. doi: 10.1101/gr.5969107
- 686 Ingimarsdóttir, M., Caruso, T., Ripa, J., Magnúsdóttir, O. B., Migliorini, M., &
687 Hedlund, K. (2012). Primary assembly of soil communities: disentangling the
688 effect of dispersal and local environment. *Oecologia*, 170(3), 745–754. doi:
689 10.1007/s00442-012-2334-8
- 690 Ji, Y., Ashton, L., Pedley, S. M., Edwards, D. P., Tang, Y., Nakamura, A., ... Yu, D. W.
691 (2013). Reliable, verifiable and efficient monitoring of biodiversity via
692 metabarcoding. *Ecology Letters*, 16(10), 1245–1257. doi: 10.1111/ele.12162
- 693 Lindo, Z., & Winchester, N. N. (2009). Spatial and environmental factors contributing
694 to patterns in arboreal and terrestrial oribatid mite diversity across spatial scales.
695 *Oecologia*, 160(4), 817–825. doi: 10.1007/s00442-009-1348-3
- 696 Magilton, M., Maraun, M., Emmerson, M., & Caruso, T. (2019). Oribatid mites reveal
697 that competition for resources and trophic structure combine to regulate the
698 assembly of diverse soil animal communities. *Ecology and Evolution*, 9(14), 8320–
699 8330. doi: 10.1002/ece3.5409
- 700 Múrria, C., Bonada, N., Vellend, M., Zamora-Muñoz, C., Alba-Tercedor, J., Sainz-
701 cantero, C. E. C. E., ... Vogler, A. P. (2017). Local environment rather than past
702 climate determines community composition of mountain stream
703 macroinvertebrates across Europe a. *Molecular Ecology*, 26(May), 6085–6099.
704 doi: 10.1111/mec.14346
- 705 Nkem, J. N., Wall, D. H., Virginia, R. A., Barrett, J. E., Broos, E. J., Porazinska, D. L.,
706 & Adams, B. J. (2006). Wind dispersal of soil invertebrates in the McMurdo Dry
707 Valleys, Antarctica. *Polar Biology*, 29(4), 346–352. doi: 10.1007/s00300-005-
708 0061-x
- 709 Oksanen, J., Blanchet, F. G., Kindt, R., Legendre, P., Minchin, P. R., O’Hara, R. B., ...
710 Wagner, H. (2013). Vegan: Community Ecology Package. R package version 2.0-
711 10. <http://cran.r-project.org/package=vegan>. *R Package Ver. 2.0–8*, p. 254.
- 712 Pearson, R. G., & Dawson, T. P. (2003). Predicting the impacts of climate change on
713 the distribution of species: are bioclimate envelope models useful? *Global Ecology
714 and Biogeography*, 12(5), 361–371. doi: 10.1046/j.1466-822X.2003.00042.x
- 715 Ramirez, K. S., Knight, C. G., De Hollander, M., Brearley, F. Q., Constantinides, B.,
716 Cotton, A., ... De Vries, F. T. (2018). Detecting macroecological patterns in
717 bacterial communities across independent studies of global soils. *Nature
718 Microbiology*, 3(2), 189–196. doi: 10.1038/s41564-017-0062-x
- 719 Ramirez, K. S., Leff, J. W., Barberán, A., Bates, S. T., Betley, J., Thomas, W., ...
720 Fierer, N. (2014). Biogeographic patterns in below-ground diversity in New York
721 City ’ s Central Park are similar to those observed globally Biogeographic patterns
722 in below-ground diversity in New York City ’ s Central Park are similar to those
723 observed globally. *Proceedings of the Royal Society B*, 281, 20141988. doi:
724 <http://dx.doi.org/10.1098/rspb.2014.1988>
- 725 Ribera, I., & Vogler, A. P. (2000). Habitat type as a determinant of species range sizes:

- 726 the example of lotic-lentic differences in aquatic Coleoptera. *Biological Journal of*
727 *the Linnean Society*, 71(1), 33–52. doi: 10.1111/j.1095-8312.2000.tb01240.x
- 728 Ricklefs, R. E. (2004). A comprehensive framework for global patterns in biodiversity.
729 *Ecology Letters*, 7(1), 1–15. doi: 10.1046/j.1461-0248.2003.00554.x
- 730 Schuppenhauer, M. M., Lehmitz, R., & Xylander, W. E. R. (2019). Slow-moving soil
731 organisms on a water highway: Aquatic dispersal and survival potential of
732 Oribatida and Collembola in running water. *Movement Ecology*, 7(1), 1–14. doi:
733 10.1186/s40462-019-0165-5
- 734 Southwood, T. R. E. (1977). Habitat, the templet for ecological strategies? *Journal of*
735 *Animal Ecology*, 46(2), 336–365.
- 736 Tang, C. Q., Leasi, F., Obertegger, U., Kieneke, a., Barraclough, T. G., & Fontaneto,
737 D. (2012). The widely used small subunit 18S rDNA molecule greatly
738 underestimates true diversity in biodiversity surveys of the meiofauna.
739 *Proceedings of the National Academy of Sciences*, 109(40), 16208–16212. doi:
740 10.1073/pnas.1209160109
- 741 Thakur, M. P., Phillips, H. R. P., Brose, U., De Vries, F. T., Lavelle, P., Loreau, M., ...
742 Cameron, E. K. (2019). Towards an integrative understanding of soil biodiversity.
743 *Biological Reviews*, 31, brv.12567. doi: 10.1111/brv.12567
- 744 Turon, X., Antich, A., Palacín, C., Præbel, K., & Wangenstein, O. S. (2019). From
745 metabarcoding to metaphylogeography: separating the wheat from the chaff.
746 *BioRxiv*, (May), 629535. doi: 10.1101/629535
- 747 Wardle, D. A. (2002). *Communities and Ecosystems: Linking the aboveground and*
748 *belowground components*. Princeton: Princeton University Press.
- 749 Widenfalk, L. A., Malmström, A., Berg, M. P., & Bengtsson, J. (2016). Small-scale
750 Collembola community composition in a pine forest soil – Overdispersion in
751 functional traits indicates the importance of species interactions. *Soil Biology and*
752 *Biochemistry*, 103, 52–62. doi: 10.1016/j.soilbio.2016.08.006
- 753 Wu, T., Ayres, E., Bardgett, R. D., Wall, D. H., & Garey, J. R. (2011). Molecular study
754 of worldwide distribution and diversity of soil animals. *Proceedings of the*
755 *National Academy of Sciences of the United States of America*, 108(43), 17720–
756 17725. doi: 10.1073/pnas.1103824108
- 757 Young, M. R., Proctor, H. C., DeWaard, J. R., & Hebert, P. D. N. (2019). DNA
758 Barcodes Expose Unexpected Diversity in Canadian Mites. *Molecular Ecology*, 0–
759 2. doi: 10.1111/mec.15292
- 760 Zinger, L., Taberlet, P., Schimann, H., Bonin, A., Boyer, F., De Barba, M., ... Chave, J.
761 (2019). Body size determines soil community assembly in a tropical forest.
762 *Molecular Ecology*, 28(3), 528–543. doi: 10.1111/mec.14919
- 763

764 **AUTHOR CONTRIBUTIONS**

765 Statement of authorship: P.A., C.A. and A.P.V. conceived the work; P.A. and C.A.
766 collected and analysed the data; P.A led the writing and all authors contributed to the
767 discussion of results and the writing.

768

769 **Table 1** Total number of haplotypes and clusters for Acari, Collembola and Coleoptera
 770 for each local setting (GRA, ALZ, CUE) at increasing levels of genetic divergence
 771 thresholds.

	haplotypes	1% lineages	2% lineages	3% lineages	4% lineages	5% lineages	6% lineages	8% lineages
GRA								
Total	1124	693	559	511	487	470	458	436
<i>Acari</i>	540	354	286	260	243	233	226	219
<i>Collembola</i>	306	172	129	113	108	104	101	94
<i>Coleoptera</i>	278	167	144	138	136	133	131	123
ALZ								
Total	1009	655	540	479	451	431	419	407
<i>Acari</i>	451	319	260	226	210	197	194	189
<i>Collembola</i>	275	155	114	94	90	87	81	77
<i>Coleoptera</i>	283	181	166	159	151	147	144	141
CUE								
Total	992	613	519	480	462	443	437	423
<i>Acari</i>	459	296	244	220	208	198	193	184
<i>Collembola</i>	273	138	117	107	101	96	95	91
<i>Coleoptera</i>	260	179	158	153	153	149	149	148

772

773

774 **FIGURE CAPTIONS**

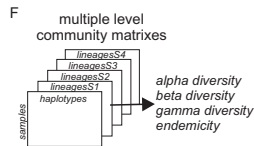
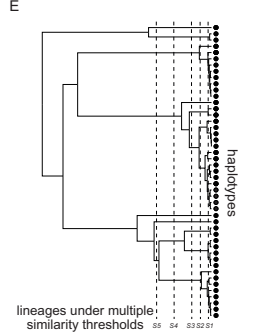
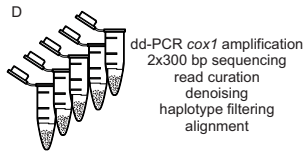
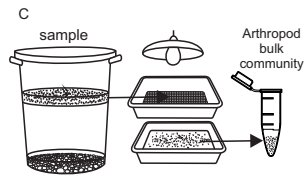
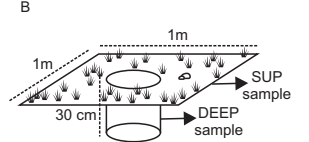
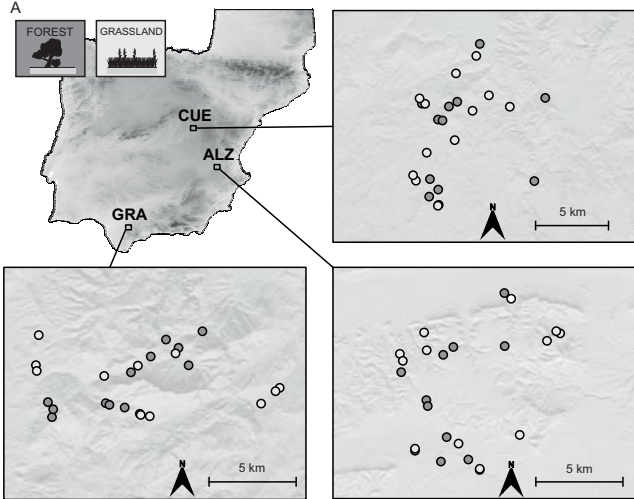
775 **Figure 1.** Sampling points in the three local settings within the Iberian Peninsula, Sierra
776 de Grazalema, (GRA), Sierra de Alatoz (ALZ) and Sierra de la Alcarria Conquense
777 (CUE). Sampling points are located within *Quercus* forest patches (dark grey) and wet
778 grassland patches (pale grey).

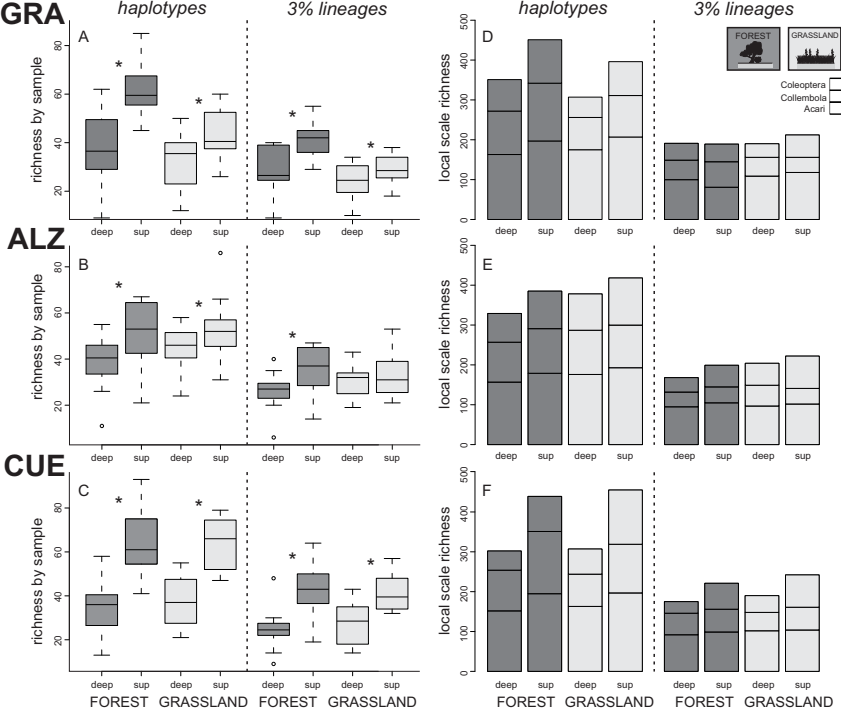
779 **Figure 2.** Richness of soil mesofauna lineages by sample (alpha diversity, A, B, C) and
780 total accumulated richness (local scale richness, D, E, F) by habitat and soil layer for the
781 three local settings (GRA, ALZ, CUE). Both measures are shown at the haplotype and
782 the 3% genetic similarity levels. Forest habitat as dark grey, grassland habitat as pale
783 gray, sup for superficial and deep for deep soil layers. Significantly different richness of
784 lineages by sample (repeated-measures ANOVA $p < 0.05$) between deep and superficial
785 communities of each habitat are indicated by asterisks within A, B, C panels. The
786 contribution of Acari, Collembola and Coleoptera to the local scale richness are shown
787 within D, E, F panels.

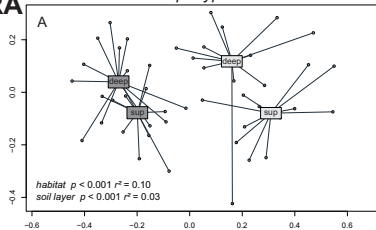
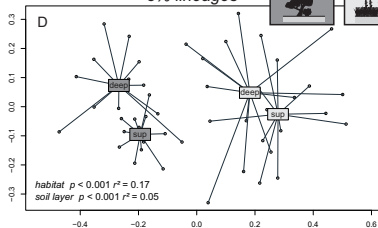
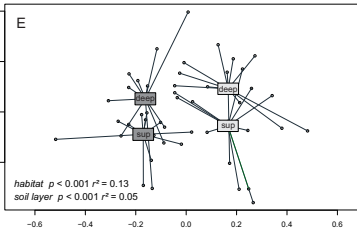
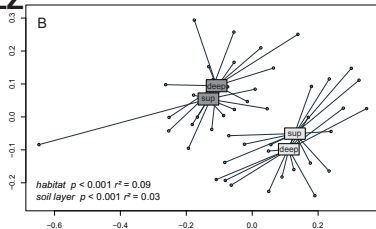
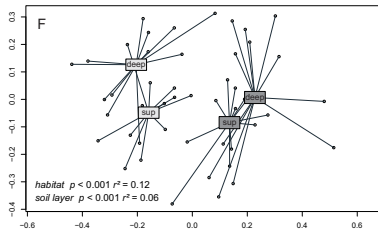
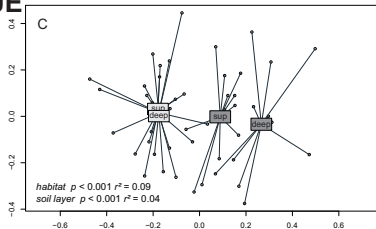
788 **Figure 3.** NMDS ordinations of the soil mesofauna samples according to the variation
789 in community composition (Simpson index, β_{sim}) within the three local settings (GRA,
790 ALZ, CUE) and at the haplotype and the 3% genetic similarity levels. Forest habitat as
791 dark grey, grassland habitat as pale grey, sup for superficial and deep for deep soil
792 layers. Explained variation (r^2) and significance (p) of each grouping factor from the
793 permutational ANOVAs over the community dissimilarity matrixes are shown.

794 **Figure 4.** Distance decay of soil mesofauna community similarity at multiple levels of
795 genetic similarity (from haplotype, black to 8% genetic similarity level, pale grey)
796 within the three local settings (GRA, ALZ, CUE) and for forest and grassland habitats.

797 **Figure 5.** Dissimilarity of soil mesofauna communities (A, B, C), regional endemicity
798 (lineages present exclusively at a single sampling point in the region divided by the total
799 number of lineages found, D, E, F) and endemicity by sampling points (lineages present
800 exclusively at a particular sampling point divided by the total number of lineages in that
801 community, G, H, I) at multiple levels of genetic similarity within the three local
802 settings (GRA, ALZ, CUE) and for forest (dark grey) and grassland (pale grey) habitats.
803 Significantly different endemicity by sampling point (Wilcoxon tests $p < 0.05$) between
804 forest and grassland communities at each hierarchical level is indicated by asterisks in
805 panels G, H, I.

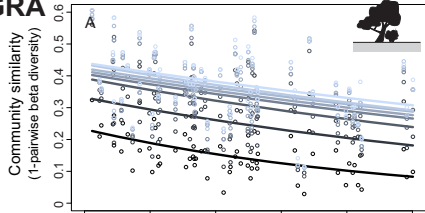




GRA*haplotypes**3% lineages***ALZ****CUE**

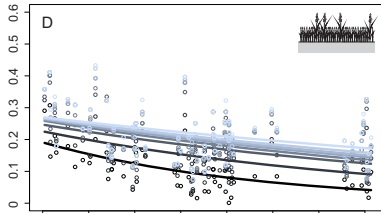
FOREST

GRA

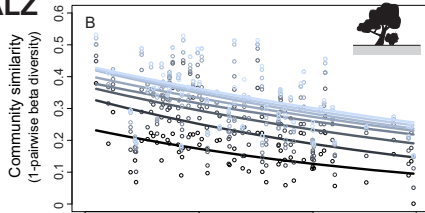


GRASSLAND

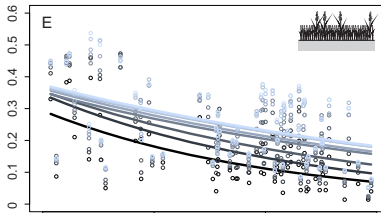
D



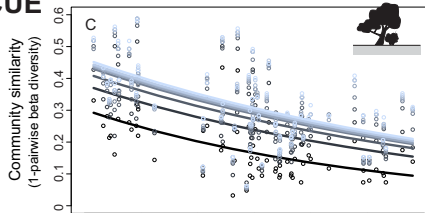
ALZ



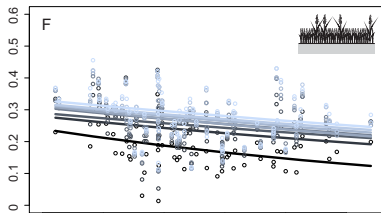
E



CUE



F



Spatial distance (km)

Spatial distance (km)

